

Effects of electron-electron interactions on the electronic Raman scattering of graphite in high magnetic fields

Y. Ma,^{1,*} Y. Kim,^{2,*} N. G. Kalugin,³ A. Lombardo,⁴ A. C. Ferrari,⁴ J. Kono,^{1,5} A. Imambekov,^{1,†} and D. Smirnov²

¹*Department of Physics and Astronomy, Rice University, Houston, Texas 77005, USA*

²*National High Magnetic Field Laboratory, Tallahassee, Florida 32310, USA*

³*Department of Materials and Metallurgical Engineering, New Mexico Tech, Socorro, New Mexico 87801, USA*

⁴*Cambridge Graphene Centre, Cambridge University, Cambridge CB3 0FA, United Kingdom*

⁵*Department of Electrical and Computer Engineering, Rice University, Houston, Texas 77005, USA*

(Received 19 April 2013; published 5 March 2014)

We report the observation of strongly temperature (T)-dependent spectral lines in electronic Raman-scattering spectra of graphite in a high magnetic field up to 45 T applied along the c axis. The magnetic field quantizes the in-plane motion, while the out-of-plane motion remains free, effectively reducing the system dimension from 3 to 1. Optically created electron-hole pairs interact with, or shake up, the one-dimensional Fermi sea in the lowest Landau subbands. Based on the Tomonaga-Luttinger liquid theory, we show that interaction effects modify the spectral line shape from $(\omega - \Delta)^{-1/2}$ to $(\omega - \Delta)^{2\alpha-1/2}$ at $T = 0$. At finite T , we predict a thermal broadening factor that increases linearly with T . Our model reproduces the observed T -dependent line shape, determining the electron-electron interaction parameter α to be ~ 0.05 at 40 T.

DOI: [10.1103/PhysRevB.89.121402](https://doi.org/10.1103/PhysRevB.89.121402)

PACS number(s): 78.30.Am, 71.70.Di, 76.40.+b, 78.20.Ls

Electron-electron (e - e) interactions become progressively more important as the system dimension is lowered. One-dimensional (1d) systems, in particular, provide model environments in which to explore interaction effects [1]. Interacting 1d electrons are expected to form an exotic electronic state of matter, the Tomonaga-Luttinger liquid (TLL) [2–5]. A strong magnetic field, B , can suppress the kinetic energy of electrons, thus enhancing the effect of interactions, as exemplified by the fractional quantum Hall effect [6–8]. For a 3d material, an applied magnetic field creates an effective 1d system along the field, ideal for a systematic study of interaction effects in a highly controllable fashion [9]. Particularly promising are 3d metals with small electron and/or hole pockets near the Fermi energy, E_F , such as bismuth [10–14] and graphite [12,15–18], where the magnetic quantum limit can be readily reached with $B \sim 10$ T.

Here we use Raman spectroscopy to study electronic states and correlations in graphite in a strong B up to 45 T applied along the c axis. The B quantizes the electronic motion in the ab plane while the motion along the c axis remains free, thus reducing the effective dimension from 3 to 1. Instead of the main Raman features related to phonons [19,20], in this work we focus on a series of electronic Raman features assigned to electronic inter-Landau-level (LL) transitions [21], whose B dependence can be explained through the Slonczewski-Weiss-McClure (SWM) model [22–24]. Each feature exhibits strongly temperature (T)-dependent shape. Our calculations show that scattering by thermally excited acoustic phonons [25–28] is too weak to explain the observations. Electron-electron interactions, on the other hand, are shown to be the cause for the observed T dependence, through the “shake-up” process, known in the problem of x-ray (or Fermi-edge) singularities [5]. Namely,

optically created electron-hole (e - h) pairs interact with, or shake up, the 1d Fermi sea in the lowest Landau subbands, resulting in line-shape deviations from single-particle densities of states (i.e., 1d Van Hove singularities). Based on the TLL theory [1–5], we show that e - e interactions modify the Van Hove singularity to the form $(\omega - \Delta)^{2\alpha-1/2}$ at 0 K, where ω is the photon frequency, Δ is the band-edge frequency, and α is a dimensionless measure of the influence of e - e interactions. At finite T , we predict a thermal broadening factor, $\Gamma(T) \propto T$. Our model reproduces the observed T -dependent line shape, determining α to be 0.016, 0.026, and 0.048, at 20, 30, and 40 T, respectively.

Raman-scattering measurements were performed on natural graphite (NGS Naturgraphit GmbH) in a back-scattering Faraday geometry in B up to 45 T, as described in Ref. [21]. The excitation beam from a 532-nm laser was focused to a spot size $< 20 \mu\text{m}$ with a power of ~ 13 mW. Most of the data were collected with a spectral resolution of $\sim 3.4 \text{ cm}^{-1}$. For high- B , low- T (≤ 10 K) measurements of the sharpest peaks, a spectral resolution of $\sim 1.9 \text{ cm}^{-1}$ was employed. The T drift over an integration time of up to 7 min, measured by a T sensor installed below the sample, was < 1 K at $T = 7$ K and < 2 K at $T \geq 180$ K.

Figure 1(a) shows Raman spectra taken at 10, 20, and 30 T at 7 K. The main band is the G peak at $\sim 1580 \text{ cm}^{-1}$, due to E_{2g} phonons [19,20]. In the presence of B , electronic Raman features appear, coming from inter-LL transitions, labeled (1,1), (2,2), \dots , etc., which we focus on in this work. Figure 1(b) shows a series of spectra taken at various B at 7 K, exhibiting electronic peaks that move with B . These peaks can be attributed to the “symmetric” inter-LL excitations in the vicinity of the K point [21,29]. The strongest, lowest-frequency transition among these is (1,1), which is from the $n = -1$ level in the valence band to the $n = 1$ level in the conduction band. Similarly, we observe the (2,2), (3,3), and (4,4) transitions; see also the zero-field in-plane dispersions and energy levels near the K point in the inset to Fig. 1(a). The symmetric inter-LL

*Y. Ma and Y. Kim equally contributed to this work.

†Deceased.

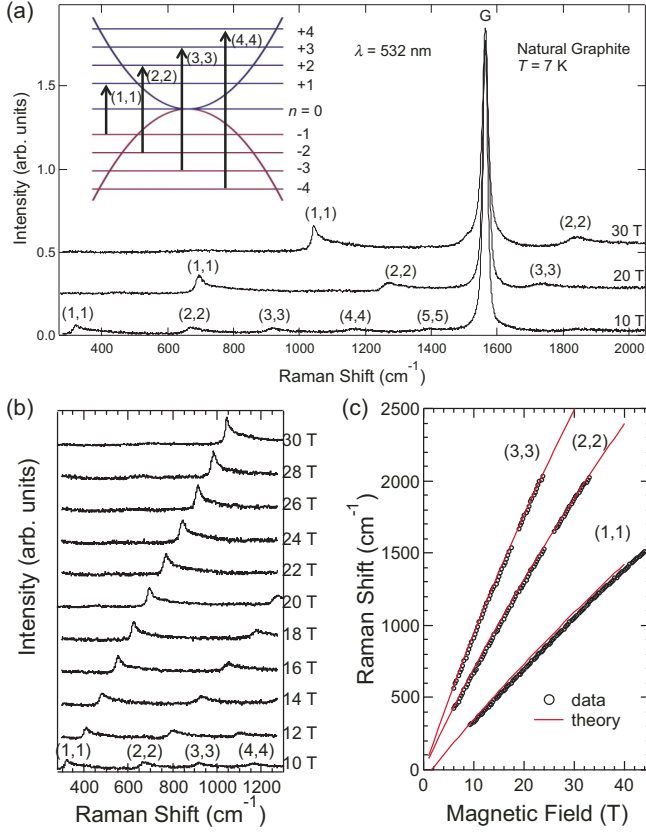


FIG. 1. (Color online) (a) Raman spectra at 10, 20, and 30 T. The feature at $\sim 1580 \text{ cm}^{-1}$ is the G peak due to the E_{2g} phonons. Inset: schematic energy-level diagram showing the transitions responsible for the electronic peaks. (b) Data taken at various B at $T = 7 \text{ K}$, showing peaks due to (1,1) through (4,4) interband transitions. (c) Peak positions of the observed (1,1), (2,2), and (3,3) transitions as a function of B , together with calculations based on the SWM model.

excitations are nonresonant Raman processes and were theoretically investigated for single-layer graphene (SLG) [30] and bilayer graphene (BLG) [31]. The peak positions of the three lowest-energy transitions are plotted against B in Fig. 1(c); they agree well with our calculations [32] (solid and dashed lines) based on the SWM model [21].

These inter-LL transitions have strong T dependence, as shown in Fig. 2, where Raman spectra at various T are plotted for (a) 20, (b) 30, and (c) 40 T. At the lowest T , the peaks exhibit sharp and asymmetric line shapes, reminiscent of a 1d Van Hove singularity, as expected from the effective dimension reduction from 3 to 1 in a B . As T increases, there is significant peak broadening and blueshift. The blueshift is expected from the thermal expansion of the carbon-carbon bonds, which changes the tight-binding parameters [28]. On the other hand, the thermal broadening cannot be explained within the tight-binding model. To quantify it, we first fit the spectra within a single-particle model using the joint density of states for interband transitions, obtained from the SWM model, with T -dependent Lorentzian broadening [32]. Figure 2(d) plots the extracted Lorentzian FWHM Γ as a function of T for 20 and 30 T. Apart from a small finite linewidth at $T = 0$,

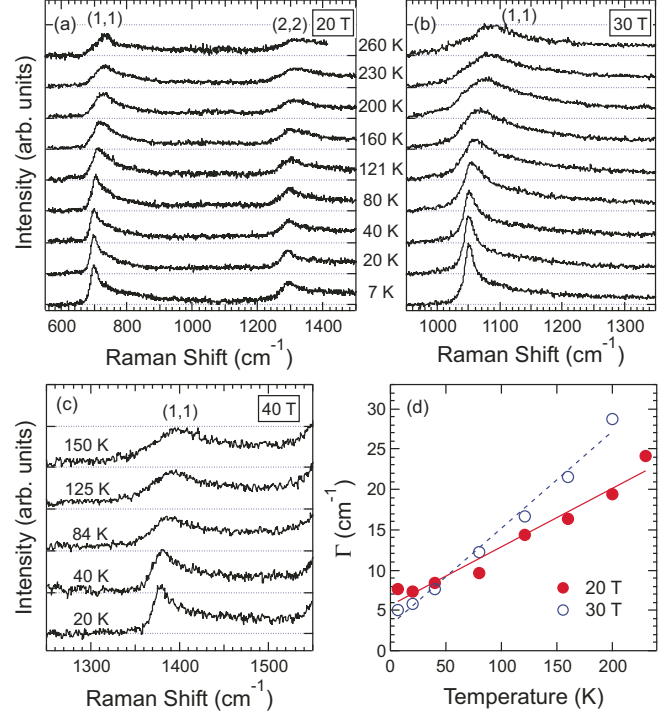


FIG. 2. (Color online) Temperature-dependent electronic Raman scattering of graphite at (a) 20 T, (b) 30 T, and (c) 40 T. (d) Temperature dependence of the broadening factor Γ of the (1,1) line at 20 T (solid circles) and 30 T (open circles). The lines are fits to the data.

$\Gamma_0 \approx 5 \text{ cm}^{-1}$, possibly due to disorder, Γ linearly depends on T .

Within the single-particle picture, T only appears in the Fermi-Dirac distribution function, but this is a negligible effect since both the initial and final states of the Raman process are far away from E_F , which resides in the $n = 0$ bands. For example, for the (1,1) transition at 30 T, the electron and hole bands are $\sim 65 \text{ meV}$ (or $\sim 750 \text{ K}$) away from E_F . Thus, we need to take into account the interactions of the photoexcited e - h pairs with some low-energy modes that would significantly change when T changes from 4 to 300 K. Specifically, since the linear- T broadening in Fig. 2(d) implies a Bose-Einstein distribution at an energy scale much smaller than $k_B T$, we only consider bosonic excitations whose characteristic energies are $\ll 100 \text{ K}$. Hence, we consider two types of low-energy modes: (i) particle-hole (p - h) excitations across E_F in the $n = 0$ bands [Fig. 3(a)] and (ii) acoustic phonons. We find that interactions with (i) explain the observed T -linear broadening while interaction with (ii) is too weak to explain it.

The magnetoelectronic Raman scattering matrix was previously calculated for SLG [30] and BLG [31] and can be readily generalized to graphite in the presence of B :

$$\hat{R} = \Lambda \sum_{\vec{k}} \Psi_n^\dagger(k_y, k_z) \Psi_{-n}(k_y, k_z), \quad (1)$$

where Λ is the scattering amplitude, k_y (k_z) are electron momenta in the ab plane (along the c axis), Ψ_n^\dagger creates an electron in the $n = 1, 2, 3, 4, \dots$ bands, and Ψ_{-n} creates a

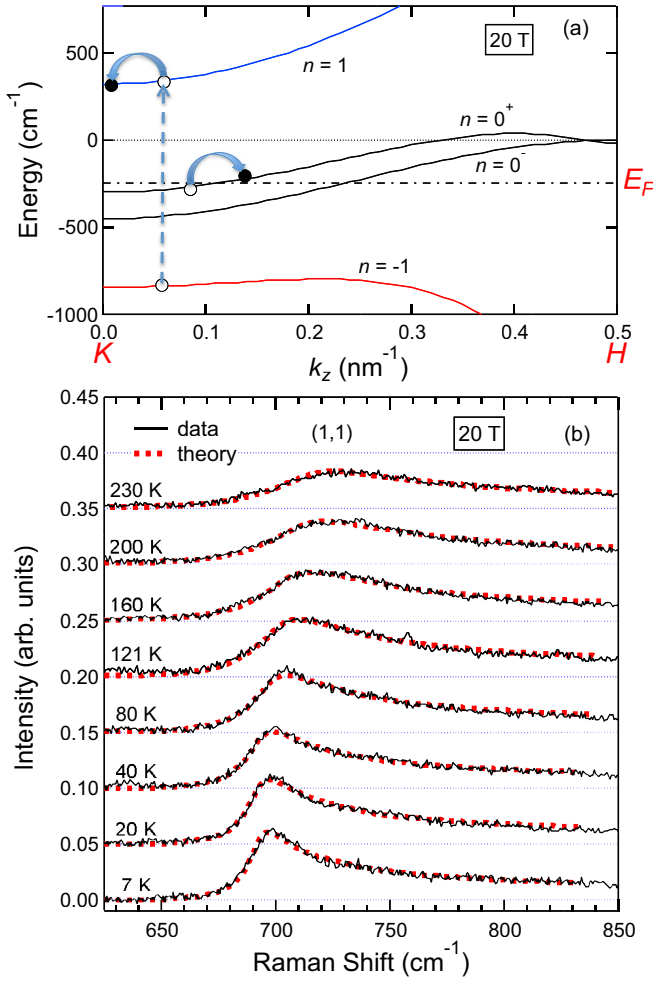


FIG. 3. (Color online) (a) The shake-up process. The (1,1) electron-hole pairs shake up the 1d Fermi sea in the lowest-energy Landau subbands, creating particle-hole pairs across E_F . (b) Temperature dependence of the line shape for the (1,1) transition at 20 T, together with fits (dashed lines) based on the model shown in (a).

hole in the $n = -1, -2, -3, -4, \dots$ bands. Both electrons and holes are massive at the bottom of the bands at the K point, i.e., $m_n \neq 0$ for all n 's, similar to BLG, but there is e - h asymmetry, i.e., $m_1 \neq m_{-1}$.

Figure 3(a) depicts the basic ingredients involved in the e - e interaction process we consider here, together with dispersions calculated via the SWM model for the $n = 0^\pm$ and ± 1 bands at 20 T. The two lowest-energy bands ($n = 0^\pm$) cross E_F , and the carriers near E_F have approximately linear dispersions. In the (1,1) process, an e - h pair is created in the $n = \pm 1$ bands, which interact with, and are thereby dressed with, multiple p - h excitations in the $n = 0^\pm$ bands near E_F . As T is raised, the thermal smearing of the Fermi edge leads to stronger interaction between the massive e - h pair and the massless p - h pairs, and the peak broadens. This type of shake-up process was theoretically studied in carbon nanotubes at 0 K [33,34]: a 1d Van Hove singularity, $(\omega - \Delta)^{-1/2}$, is predicted to become $(\omega - \Delta)^{2\alpha-1/2}$ with $\alpha \sim 0.1$ once the shake-up process is taken into account.

We describe the $n = 0^-$ electrons as a TLL with the Hamiltonian [1–4] given by

$$H_0^c = v_F \int dz [\psi_R^\dagger i \partial_z \psi_R - \psi_L^\dagger i \partial_z \psi_L], \quad (2)$$

where v_F is the Fermi velocity and $\psi_{R(L)}^\dagger$ creates a particle near the right (left) Fermi point. The $n = 0^+$ band can be described by a similar Hamiltonian but with a different v_F . By approximating the energy dispersion near E_F as $E \propto k_z$, we can rewrite Eq. (2) via bosonization as

$$H_0^c = \frac{v_F}{2\pi} \int dz [(\nabla\phi)^2 + (\nabla\theta)^2], \quad (3)$$

where $\nabla\phi = -2\pi[\rho_R + \rho_L]$, $\nabla\theta = 2\pi[\rho_R - \rho_L]$, and ρ_R (ρ_L) is the density operator for right-moving (left-moving) electrons.

We assume that the photogenerated electrons ($n = 1$) and holes ($n = -1$) interact with the $n = 0^-$ conduction electrons separately. For the $n = 1$ band, where electrons are massive, we can treat the electrons through

$$H_1 = \int dz \Psi_1^\dagger \left[-\frac{1}{2m} \partial_z^2 + \Delta_1 \right] \Psi_1, \quad (4)$$

where Δ_1 is the band-edge frequency and Ψ_1^\dagger (Ψ_1) is the creation (annihilation) operator for the $n = 1$ band. We also assume that the interaction Hamiltonian only involves the total charge density, thus neglecting any backscattering and umklapp scattering:

$$H_{\text{int}} = \frac{V}{2} \int dz \left[\Psi_1^\dagger \Psi_1 - \frac{1}{2\pi} \nabla\phi \right]^2. \quad (5)$$

We write the effective Hamiltonian for the system as the sum of Eqs. (3)–(5): $H = H_0^c + H_1 + H_{\text{int}}$.

The diagonalization of the Hamiltonian is a unitary transformation $U^\dagger H U$ and has been previously solved by many authors [33–36]:

$$U^\dagger = \exp \left[-i \frac{\gamma^+}{\pi} \int dy \theta(y) \Psi_1^\dagger(y) \Psi_1(y) \right]. \quad (6)$$

Under this transformation, the original interacting system can be mapped to a noninteracting one, and the massive-electron operator acquires an additional string operator, $\Psi_1(z) = \exp[-i\gamma^+\theta(z)/\pi] \tilde{\Psi}_1(z)$, where $\tilde{\Psi}_1^\dagger$ creates a free electron in the $n = 1$ band. The massive $n = 1$ electron then gets dressed by the additional string operator, i.e., the $n = 0^-$ conduction electrons adiabatically adjust to the massive electrons. Similarly, we can obtain a dressed expression for the massive hole.

The spectral function can be obtained by calculating the imaginary part of the retarded Green's function [5],

$$G^R(z, t) \equiv -i\theta(t) \langle [\Psi_{-1}^\dagger(z, t) \Psi_1(z, t), \Psi_1^\dagger(0, 0) \Psi_{-1}(0, 0)] \rangle. \quad (7)$$

At zero T , Eq. (7) can be evaluated directly in real space. However, at finite T , one has to follow a different route. As the Green's function for the massive electron/hole and that for the conduction electrons are both straightforward to obtain,

the total Green's function can be written as a convolution of three Green's functions,

$$\begin{aligned} G^R(z, t) &\approx -i\theta(t)[-iG_{-1}^<(-z, -t)][iG_1^>(z, t)]F(z, t), \\ G^R(0, \omega) &= -i \int \prod \frac{dp_i}{2\pi} \frac{d\omega_i}{2\pi} G^0(p_2, \omega_2) F(p_1, \omega_1) \\ &\quad \times \delta(0 - p_1 - p_2) \delta(\omega - \omega_1 - \omega_2), \\ G^0(p, \omega) &= \int \frac{dp_1}{2\pi} \int \frac{d\omega_1}{2\pi} G_1^>(p_1, \omega_1) \\ &\quad \times G_{-1}^<(p_1 - p, \omega_1 - \omega), \end{aligned} \quad (8)$$

where

$$F(z, t) = \langle \exp[-i\gamma\theta(x, t)] \exp[i\gamma\theta(0, 0)] \rangle. \quad (9)$$

We can express the spectral function in a universal form as

$$A(\omega) = \Lambda T^{2\alpha-0.5} \tilde{F}\left(\frac{\omega/T}{4\pi}, \alpha\right), \quad (10)$$

where

$$\begin{aligned} \tilde{F}(z, t) &= \sum_{n=0}^{\infty} \sum_{m=0}^{\infty} B[n + \alpha, 1 - \alpha] B[m + \alpha, 1 - \alpha] \\ &\quad \times \text{Re} \left[\frac{(2i)^{2\alpha}}{\sqrt{z - \frac{i}{2}(m + n + \alpha)}} \right]. \end{aligned} \quad (11)$$

In Eq. (11) there are two dimensionless parameters: ω/T and α . The first parameter implies that the spectral width linearly depends on T for a fixed α . The meaning of α can be understood by studying the $T = 0$ asymptotic behavior of Eq. (11), and comparing it with the previous zero- T results [33,34]. It then becomes clear that

$$A(\omega) \propto \frac{\Theta(\omega - \Delta)}{(\omega - \Delta)^{2\alpha-1/2}}, \quad (12)$$

where Θ is the Heaviside function. For metallic carbon nanotubes, α was estimated to be ~ 0.1 [33,34]. To fit our experimental data with our model, we use the true band structure instead of a parabolic approximation, by fitting the tail up to $\sim 0.2(\pi/c)$ from the K point. Figure 3(b) shows how well our model fits the data, determining $\alpha(20 \text{ T}) \approx 0.016$, $\alpha(30 \text{ T}) \approx 0.026$, and $\alpha(40 \text{ T}) \approx 0.048$. These values are smaller than the value estimated for nanotubes, as expected, but there is a trend that α increases with B , as this tends to make the system more 1d.

We now consider acoustic phonons, which can also couple to the massive electrons and holes. We use the approximation that in-plane and out-of-plane modes are separated. This approximation leads to a slight numerical modification of the following equations but greatly simplifies our understanding of electron-acoustic phonon interactions in graphite. The properties of acoustic phonons can be described by five elastic constants [37]: $C_{11} = 1109 \text{ GPa}$, $C_{66} = 485 \text{ GPa}$, $C_{33} = 38.7 \text{ GPa}$, $C_{13} = 0 \text{ GPa}$, and $C_{44} = 5 \text{ GPa}$. Unlike the case of optical phonons [19,26,38,39], coupling with acoustic phonons vanishes at the Γ point since the electron-acoustic-phonon interaction Hamiltonian $H_{\text{ep}} \sim \sqrt{q}$ [25,40,41], where q is the phonon wavenumber. We then evaluate the thermal

broadening of Raman peaks by calculating the imaginary part of the self-energy:

$$\begin{aligned} H_{\text{ep}} &= \sum_{\vec{k}, \vec{k}', \vec{q}} g_{\vec{q}} h(\vec{q}) \Psi_1^\dagger(k_y + q_y, k_z + q_z) \Psi_1(k_y, k_z) (b_{-\vec{q}}^\dagger + b_{\vec{q}}), \\ g_{\vec{q}} &= \frac{\eta \kappa q \sin \theta}{2} \sqrt{\frac{\hbar}{2NM\omega_{\vec{q}}}} \frac{\sqrt{2}}{2} \frac{\Delta_B^2}{\Gamma\gamma_1}, \\ h(\vec{q}) &= \left(4 - 2l_B^2 q^2 \sin^2 \theta + \frac{l_B^4 q^4 \sin^4 \theta}{8} \right) e^{-(l_B^2 q^2 \sin^2 \theta)/4}, \end{aligned} \quad (13)$$

where $l_B = (\hbar/eB)^{1/2}$ is the magnetic length, $\eta \sim 2$, and $\kappa \sim 1/3$ [26]. To first order, we estimate the scattering rate through Fermi's "golden rule":

$$W_i = \frac{2\pi}{\hbar} \sum_f |\langle f | H_{\text{ep}} | i \rangle|^2 \delta(E_i - E_f). \quad (14)$$

When the momentum transfer during the scattering process is small (i.e., $vq \ll k_B T$), the phase space for phonon modes is $q^2(\frac{1}{e^{vq/kT}} + \frac{1}{2} \pm \frac{1}{2}) \sim qT \rightarrow 0$, and when the momentum transfer is large, the overlap between initial and final states has a factor $\exp(-q^2 l_B^2)$. For $B = 30 \text{ T}$, $l_B \sim 5 \text{ nm}$, which is at least one order larger than the carbon-carbon bond length. Thus, the contribution to scattering drops exponentially as the phonon modes move away from the Γ point (or, equivalently, with increasing energy). The calculated momentum-dependent scattering rate is then given by

$$\begin{aligned} W(k_z) &= \Lambda' \int_0^\pi d\theta \frac{\tilde{q}^2 \sin^3 \theta}{\sqrt{\sin^2 \theta + \frac{V_4^2}{V_1^2} \cos^2 \theta}} \frac{h^2(q, \theta)}{\cos^2 \theta} \\ &\quad \times \left(n_{\omega_{\vec{q}}} + \frac{1}{2} \pm \frac{1}{2} \right), \end{aligned} \quad (15)$$

where

$$\begin{aligned} \tilde{q} &= \frac{2ml_B V_1}{\hbar} \frac{\hbar k_z}{mV_1} \cos \theta \mp \sqrt{\sin^2 \theta + V_4^2/V_1^2 \cos^2 \theta}, \\ \hbar\Lambda' &= \frac{\eta^2 \kappa^2}{16\pi} \frac{m}{M} \frac{V_{\text{unit}}}{l_B^3} \frac{\Delta_B^2}{\gamma_1^2} \frac{\sqrt{2}v}{V_1} \Delta_B \approx 4.1 \times 10^{-6} \text{ cm}^{-1}. \end{aligned}$$

This value leads to $W(k_z) \sim 10^{-4} \text{ cm}^{-1}$ at 30 T and 200 K, too small to explain the observed broadening, which requires the scattering rate to be $\sim 10 \text{ cm}^{-1}$. There are two reasons for the small $\hbar\Lambda'$: one is $m/M \sim 10^{-3}$, and the other is V_{unit}/l_B^2 . The latter, i.e., the magnetic length suppression, is a unique aspect of this work, made possible by a high B .

In summary, we studied electronic Raman scattering in graphite in a strong magnetic field up to 45 T, applied along the c axis. We observe a series of spectral lines, ascribed to inter-Landau-subband transitions, and each line exhibits strongly T -dependent line shape. We developed a microscopic model based on the Tomonaga-Luttinger theory, with which we show that the shake-up process can explain the observed results. Specifically, electron-electron interactions modify the Van Hove singularity to the form $(\omega - \Delta)^{2\alpha-1/2}$ at $T = 0$. Our model accurately reproduces the observed T -dependent line shape, determining α to be 0.016, 0.026, and 0.048, at 20, 30, and 40 T, respectively.

We acknowledge funding from NHMFL UCGP-5068, DOE/BES DE-FG02-07ER46451, NSF (Grant No. DMR-1006663), DOE BES Program (Grant No. DE-FG02-06ER46308), the Robert A. Welch Foundation (Grant No. C-1509), a Royal Society Wolfson Research Merit Award, the Eu-

ropean Research Council Grants NANOPOTS and Hetero2D, EU Grants CareRAMM and Graphene Flagship (Contract no. 604391), EPSRC Grants EP/K01711X/1 and EP/K017144/1, Nokia Research Centre, Cambridge. We thank M. S. Foster, E. G. Mishchenko, and O. A. Starykh for valuable discussions.

-
- [1] T. Giamarchi, *Quantum Physics in One Dimension* (Oxford University Press, Oxford, 2004).
 - [2] S. Tomonaga, *Prog. Theor. Phys.* **5**, 544 (1950).
 - [3] J. M. Luttinger, *J. Math. Phys.* **4**, 1154 (1963).
 - [4] F. D. M. Haldane, *Phys. Rev. Lett.* **47**, 1840 (1981).
 - [5] G. D. Mahan, *Many-Particle Physics*, 3rd ed. (Kluwer Academic/Plenum, New York, 2000).
 - [6] D. C. Tsui, H. L. Stormer, and A. C. Gossard, *Phys. Rev. Lett.* **48**, 1559 (1982).
 - [7] X. Du, I. Skachko, F. Duerr, A. Luican, and E. Y. Andrei, *Nature (London)* **462**, 192 (2009).
 - [8] K. I. Bolotin, F. Ghahari, M. D. Shulman, H. L. Stormer, and P. Kim, *Nature (London)* **462**, 196 (2009).
 - [9] C. Biagini, D. L. Maslov, M. Y. Reizer, and L. I. Glazman, *Europhys. Lett.* **55**, 383 (2001).
 - [10] S. Mase and T. Sakai, *J. Phys. Soc. Jpn.* **31**, 730 (1971).
 - [11] S. Nakajima and D. Yoshioka, *J. Phys. Soc. Jpn.* **40**, 328 (1976).
 - [12] X. Du, S.-W. Tsai, D. L. Maslov, and A. F. Hebard, *Phys. Rev. Lett.* **94**, 166601 (2005).
 - [13] K. Behnia, L. Balicas, and Y. Kopelevich, *Science* **317**, 1729 (2007).
 - [14] L. Li, J. G. Checkelsky, Y. S. Hor, C. Uher, A. F. Hebard, R. J. Cava, and N. P. Ong, *Science* **321**, 547 (2008).
 - [15] Y. Iye, P. M. Tedrow, G. Timp, M. Shayegan, M. S. Dresselhaus, G. Dresselhaus, A. Furukawa, and S. Tanuma, *Phys. Rev. B* **25**, 5478 (1982).
 - [16] D. Yoshioka and H. Fukuyama, *J. Phys. Soc. Jpn.* **50**, 725 (1981).
 - [17] D. V. Khveshchenko, *Phys. Rev. Lett.* **87**, 206401 (2001).
 - [18] Y. Kopelevich, B. Raquet, M. Goiran, W. Escoffier, R. R. da Silva, J. C. Medina Pantoja, I. A. Luk'yanchuk, A. Sinchenko, and P. Monceau, *Phys. Rev. Lett.* **103**, 116802 (2009).
 - [19] A. C. Ferrari, *Solid State Commun.* **143**, 47 (2007).
 - [20] A. C. Ferrari and D. M. Basko, *Nat. Nano* **8**, 235 (2013).
 - [21] Y. Kim, Y. Ma, A. Imambekov, N. G. Kalugin, A. Lombardo, A. C. Ferrari, J. Kono, and D. Smirnov, *Phys. Rev. B* **85**, 121403(R) (2012).
 - [22] J. W. McClure, *Phys. Rev.* **108**, 612 (1957).
 - [23] J. C. Slonczewski and P. R. Weiss, *Phys. Rev.* **109**, 272 (1958).
 - [24] J. W. McClure, *Phys. Rev.* **119**, 606 (1960).
 - [25] L. M. Woods and G. D. Mahan, *Phys. Rev. B* **61**, 10651 (2000).
 - [26] H. Suzuura and T. Ando, *Phys. Rev. B* **65**, 235412 (2002).
 - [27] J. Jiang, R. Saito, A. Grüneis, G. Dresselhaus, and M. S. Dresselhaus, *Chem. Phys. Lett.* **392**, 383 (2004).
 - [28] N. Mounet and N. Marzari, *Phys. Rev. B* **71**, 205214 (2005).
 - [29] P. Kossacki, C. Faugeras, M. Kühne, M. Orlita, A. A. L. Nicolet, J. M. Schneider, D. M. Basko, Y. I. Latyshev, and M. Potemski, *Phys. Rev. B* **84**, 235138 (2011).
 - [30] O. Kashuba and V. I. Fal'ko, *Phys. Rev. B* **80**, 241404 (2009).
 - [31] M. Mucha-Kruczyński, O. Kashuba, and V. I. Fal'ko, *Phys. Rev. B* **82**, 045405 (2010).
 - [32] See Supplemental Material at <http://link.aps.org/supplemental/10.1103/PhysRevB.89.121402> for details of our data analysis and theoretical calculation methods.
 - [33] L. Balents, *Phys. Rev. B* **61**, 4429 (2000).
 - [34] E. G. Mishchenko and O. A. Starykh, *Phys. Rev. Lett.* **107**, 116804 (2011).
 - [35] A. Imambekov and L. I. Glazman, *Phys. Rev. Lett.* **102**, 126405 (2009).
 - [36] A. Imambekov and L. I. Glazman, *Science* **323**, 228 (2009).
 - [37] A. Bosak, M. Krisch, M. Mohr, J. Maultzsch, and C. Thomsen, *Phys. Rev. B* **75**, 153408 (2007).
 - [38] T. Ando, *J. Phys. Soc. Jpn.* **75**, 124701 (2006).
 - [39] A. C. Ferrari, J. C. Meyer, V. Scardaci, C. Casiraghi, M. Lazzeri, F. Mauri, S. Piscanec, D. Jiang, K. S. Novoselov, S. Roth, and A. K. Geim, *Phys. Rev. Lett.* **97**, 187401 (2006).
 - [40] N. Bonini, M. Lazzeri, N. Marzari, and F. Mauri, *Phys. Rev. Lett.* **99**, 176802 (2007).
 - [41] P. Giura, N. Bonini, G. Creff, J. B. Brubach, P. Roy, and M. Lazzeri, *Phys. Rev. B* **86**, 121404 (2012).